

2018-09-01

Relationship between mineralogy and minor element partitioning in limpets from an Ischia CO₂ vent site provides new insights into their biomineralization pathway

Langer, G

<http://hdl.handle.net/10026.1/12309>

10.1016/j.gca.2018.02.044

Geochimica et Cosmochimica Acta

Elsevier

All content in PEARL is protected by copyright law. Author manuscripts are made available in accordance with publisher policies. Please cite only the published version using the details provided on the item record or document. In the absence of an open licence (e.g. Creative Commons), permissions for further reuse of content should be sought from the publisher or author.



Relationship between mineralogy and minor element partitioning in limpets from an Ischia CO₂ vent site provides new insights into their biomineralization pathway

Gerald Langer^{a,b,*}, Aleksey Sadekov^{b,1}, Gernot Nehrke^c, Cecilia Baggini^d,
Riccardo Rodolfo-Metalpa^e, Jason M. Hall-Spencer^{d,f}, Emilio Cuoco^g, Jelle Bijma^c,
Henry Elderfield^b

^a *The Marine Biological Association of the United Kingdom, The Laboratory, Citadel Hill, Plymouth, Devon PL1 2PB, UK*

^b *Department of Earth Sciences, Cambridge University, Cambridge, UK*

^c *Marine Biogeosciences, Alfred-Wegener-Institut Helmholtz-Zentrum für Polar- und Meeresforschung, Bremerhaven, Germany*

^d *Marine Biology and Ecology Research Centre, University of Plymouth, Plymouth, UK*

^e *Institut de Recherche pour le Développement - IRD, UMR 250, Nouméa, New Caledonia*

^f *Shimoda Marine Research Centre, Tsukuba University, Japan*

^g *Department of Environmental, Biological and Pharmaceutics Sciences and Technology, Second University of Naples, Caserta, Italy*

Received 10 April 2017; accepted in revised form 28 February 2018; available online xxxx

Abstract

It has long since been noted that minor element (Me) partitioning into biogenic carbonates is sometimes different from Me partitioning into inorganically precipitated carbonates. The prime example is the partitioning coefficient, which might be lower or even higher than the one of inorganically precipitated carbonate. Such a difference is usually termed “vital effect” and is seen as indicative of a biologically modified minor element partitioning. Over the last three decades interest in conceptual biomineralization models compatible with minor element and isotope fractionation has been steadily increasing. However, inferring features of a biomineralization mechanism from Me partitioning is complicated, because not all partitioning coefficients show vital effects in every calcium carbonate producing organism. Moreover, the partitioning coefficient is not the only aspect of Me partitioning. Other aspects include polymorph specificity and rate dependence. Patellogastropod limpets are ideally suited for analysing Me partitioning in terms of biomineralization models, because they feature both aragonitic and calcitic shell parts, so that polymorph specificity can be tested. In this study, polymorph-specific partitioning of the minor elements Mg, Li, B, Sr, and U into shells of the patellogastropod limpet *Patella caerulea* from within and outside a CO₂ vent site at Ischia (Italy) was investigated by means of LA-ICP-MS. The partitioning coefficients of U, B, Mg, and Sr (in aragonite) differed from the respective inorganic ones, while the partitioning coefficients of Li and Sr (in calcite) fell within the range of published values for inorganically precipitated carbonates. Polymorph specificity of Me partitioning was explicable in terms of inorganic precipitation in the case of Sr and Mg, but not Li and B. Seawater carbon chemistry did not have the effect on B partitioning that was expected on the basis of data on inorganic precipitates and foraminifera. Carbon chemistry did affect Mg (in aragonite) and Li, but only the effect on Mg was explicable in terms of calcification rate. On the one hand, these results show that Me partitioning in *P. caerulea* is incompatible with a direct precipitation of shell calcium carbonate from the extrapallial fluid. On the other hand, our results are compatible with precipitation from a microenvironment formed by the mantle.

* Corresponding author at: The Marine Biological Association of the United Kingdom, The Laboratory, Citadel Hill, Plymouth, Devon PL1 2PB, UK.

E-mail address: gerlan@mba.ac.uk (G. Langer).

¹ Present Address: School of Earth Sciences, University of Western Australia, Perth, Australia.

<https://doi.org/10.1016/j.gca.2018.02.044>

0016-7037/© 2018 Elsevier Ltd. All rights reserved.

Such a microenvironment was proposed based on data other than Me partitioning. This is the first study which systematically employs a multi-element, multi-aspect approach to test the compatibility of Me partitioning with different conceptual biomineralization models.

© 2018 Elsevier Ltd. All rights reserved.

Keywords: Mollusc biomineralisation; Minor element fractionation; Shell mineralogy

1. INTRODUCTION

For decades, the element and isotope fractionation into biogenic marine calcium carbonate (biominerals) has been used to reconstruct environmental conditions e.g. temperature and seawater chemistry (Elderfield et al. 2000, Lea 2014). These reconstructions are complicated by the biomineralization processes that lead to the formation of biominerals, e.g., the calcified structures of foraminifera, corals, and gastropods. To understand if and how other parameters than the target parameter affect proxy relationships such as those between temperature and the Mg/Ca ratio or between pH and the boron isotopic composition, it is necessary to consider these biomineralisation mechanisms. Consequently the interest in biomineralisation models as an aid to proxy understanding has been steadily increasing over the last two decades. These models are usually based on a variety of widely differing aspects, e.g., physiology, biochemistry, anatomy, ultrastructure, and the fractionation of elements itself. It has become increasingly clear that biomineralisation models, which explain minor element and isotope fractionation, differ between groups of marine calcifiers and sometimes even between species within groups.

At first glance calcification in the marine environment seems to be straightforward because seawater contains ample calcium and carbonate ions. However, most marine organisms do not precipitate calcium carbonate directly from seawater. Instead, calcification takes place in a confined space separated from seawater. This site of calcification is either extracellular or intracellular. In either case, a transport of calcium and carbonate from seawater to the calcification site is required. This transport will include ions other than calcium and carbonate and is likely to introduce an element as well as an isotope fractionation, because various elements and their isotopes might have different transport characteristics. The precise transport pathways for many organisms are still a matter of debate but three different ways of transporting the building blocks of the carbonate biomineral seem to describe the fundamental processes, namely paracellular, vacuolar, and transmembrane transport. Direct seawater transport to the calcification site is assumed to account for trace element partitioning into coral skeletons (Gagnon et al. 2012). This direct transport could be paracellular or vacuole mediated (Erez and Braun, 2007; Tambutté et al., 2012; Mass et al., 2017). Seawater transport by means of vacuoles was also suggested for sea urchins and foraminifera (Bentov et al., 2009; Vidavsky et al., 2016). Since some foraminifera exclude more magnesium from their shell than inorganic precipitation from seawater does, it was suggested that the ionic composition of the seawater inside the vacuoles is

altered by means of active ion transport mechanisms (Erez, 2003). These active (and passive) transmembrane transport mechanisms could also transport calcium and other ions from seawater without the need for bulk seawater endocytosis. It was recently suggested that foraminifera use transmembrane ion transport as their main calcium source and that seawater vacuolisation plays a secondary role (Nehrke et al., 2013). However, there seems to be consensus that coccolithophores take up calcium across the plasmamembrane, although they might employ vesicles to accumulate and intracellularly transport it to the coccolith vesicle (Taylor et al., 2017). In marine molluscs, the initial idea about calcium transport represents probably the least complicated scenario. It was suggested that shell calcium carbonate is directly precipitated from the extrapallial fluid (EPF) (Crenshaw, 1972; Misogianes and Chasteen, 1979). The EPF is essentially seawater in ionic composition and therefore contains ample calcium (Crenshaw, 1972; Misogianes and Chasteen, 1979; Coimbra et al., 1988; Heinemann et al., 2012). However, in terrestrial molluscs all calcium used in shell construction is taken up with the food and therefore the calcium has to be extracted from the food and transported through various tissues to the calcification site. This scenario is comparatively complicated because it includes many transport steps. Such a multi-step ion transport is not necessarily confined to terrestrial molluscs, but might be widespread among marine species too. In the last three decades it was repeatedly suggested that molluscs do not precipitate shell calcium carbonate directly from the EPF, but that at the site of shell formation the mantle epithelium is in close contact with the shell surface, effectively blocking any contact of the EPF with the shell surface (Simkiss and Wilbur, 1989; Beniash et al., 1999; Addadi et al., 2006; Suzuki et al., 2009; Cuif et al., 2011). This requires ion transport across the mantle epithelium. Some authors suggested that calcium might be transported as amorphous calcium carbonate granules in vesicles (Addadi et al., 2006; Marin et al., 2012; Xiang et al., 2014) and amorphous precursors of calcite or aragonite were reported for other calcifiers such as urchins (Beniash et al., 1999). Hence the initial idea of a direct precipitation of aragonite or calcite from a seawater like EPF seems too simple a scenario and a more complicated picture including ion transport and mineral transformation emerges, which also explains much better how molluscs can form their intricate shell structures (Bowerbank, 1844).

Even this brief survey of ion transport mechanisms related to biomineralisation makes clear that models based on data from different species are in danger of being unrealistic. It is often not obvious why the fractionation behaviour of a particular element differs between species. For instance, boron and its isotopes have been used to

reconstruct seawater carbon chemistry, but this requires species specific calibrations. In foraminifera boron is a good indicator of carbon chemistry, and initially corals seemed similarly promising (Hoenisch et al., 2004; Foster et al., 2008b). A more recent study suggested a difference between aragonitic and calcitic corals (McCulloch et al., 2012). The authors inferred a “mineralogical control on biological pH up-regulation”. This inference is not without difficulty because a calcitic species was compared with aragonitic ones and so the polymorph difference was by no means the only difference between these organisms. Both foraminifera and coccolithophores are calcitic but boron in the latter does not seem a good indicator of seawater carbon chemistry (Stoll et al., 2012). Little work was done on molluscs but boron in bivalves does not seem to be a reliable carbon chemistry proxy (McCoy et al., 2011; Heinemann et al., 2012).

With respect to understanding element fractionation in terms of biomineralisation mechanisms the focus on one single element and a number of different species is of limited value. As the example of boron shows it might not be clear whether a difference in element fractionation can be attributed to a particular feature of the organism’s calcification mechanism, e.g. the choice of polymorph. Moreover, a particular feature of an element’s fractionation behaviour might not be easily related to biomineralisation mechanisms. For instance, the Mg/Ca ratio has been used as a temperature proxy in foraminifera, ostracoda, and corals (Lea, 2014). These groups of organisms clearly have different biomineralisation mechanisms. In order to bring biomineralisation mechanisms and element fractionation effectively together, it is advantageous to focus on a single organism and more than one element. In this study we therefore investigate the incorporation of Mg, Sr, Li, B, and U in shells of the patellogastropod limpet *Patella caerulea* (Linnaeus, 1758). We used *P. caerulea*, because patellogastropod limpets feature both aragonitic and calcitic shell parts (Hedegaard et al., 1997). Our LA-ICPMS measurements were performed on shells for which the spatial polymorph distribution had been well-documented in an earlier study (Langer et al., 2014). This made a comparison of the minor elements (Me) composition of the two polymorphs possible. These shells were collected within and outside a CO₂ vent site off Ischia. The Ischia CO₂ vent site has a large range in carbon chemistry (Rodolfo-Metalpa et al., 2011). This allowed us to analyse the influence of seawater carbon chemistry on element fractionation, which is particularly interesting for elements such as B and U, because they display a carbon chemistry dependent speciation in seawater (McClaine et al., 1955; Dickson, 1990).

2. MATERIAL AND METHODS

2.1. Study site and sampling

The study site was off the east coast of Ischia (40° 43.81'N, 13°57.98'E) at the low water mark. Gas emissions from the seabed in this area are composed of 90–95% CO₂, 3–6% N₂, 0.6–0.8% O₂, 0.2–0.8% CH₄ and 0.08–0.1% Ar, without toxic sulphur compounds (Hall-Spencer et al.,

2008). Shallow water CO₂ seeps are now being used extensively as a natural laboratory to investigate the ecosystem effects of ocean acidification (Sunday et al., 2017). Gas fluxes were measured during 2006–2007, and no seasonal, tidal or diurnal variation in gas flow rates was detected, while pH and saturation states of aragonite and calcite varied with sea state, being lowest on calm days, and showed large decreases as pCO₂ increased proceeding towards the vent sites (Hall-Spencer et al., 2008). *Patella caerulea* specimens were collected from two low pH sites (L-shells), and from a control site (N-shells) in December 2009 and analysed for polymorph distribution (Langer et al., 2014). Temperature, pH and TA were measured from September to December 2009, and the other carbonate chemistry parameters were calculated from them. The two low pH sites had a mean pH of 6.46 ± 0.35 (mean \pm S.D.) and 6.51 ± 0.38 respectively, while the control site had a mean pH of 8.03 ± 0.05 (Rodolfo-Metalpa et al., 2011; Langer et al., 2014).

2.2. Raman spectroscopy

The spatial distribution of aragonite and calcite within the investigated shell was determined in a previous study (Langer et al., 2014) by means of confocal Raman microscopy. Raman imaging was done using a WITec alpha 300 R (WITec GmbH, Germany) confocal Raman microscope. For imaging a Raman spectrum was acquired every 10 μ m. For details please refer to Langer et al. (2014).

2.3. LA-ICPMS

Me/Ca ratios of shells were measured using Laser Ablation-Inductively Coupled Plasma Mass Spectrometry (LA-ICPMS) system at the Department of Earth Science at University of Cambridge. This analytical technique employs an Analyte G2 excimer laser (Teledyne Photon Machines Inc) coupled with Thermo i-CapQ ICPMS. The isotopes ⁷Li, ¹¹B, ²⁵Mg, ²⁷Al, ⁴³Ca, ⁵⁵Mn, ⁵⁶Fe, ⁶⁶Zn, ⁸⁸Sr, ²³⁸U were measured along the laser profile tracks. Laser Ablation system was optimised for high spatial resolution using aperture slit of $5 \times 100 \mu$ m aligned to direction of the shell growth and 6 Hz frequency with 1.8 J/cm^2 laser fluence. The scan speed of the laser along the tracks was set at $2 \mu\text{m/s}$, resulting in spatial resolution of approximately one Me/Ca measurement per $1 \mu\text{m}$ of the shell extension. Prior to the measurements approximately top $1 \mu\text{m}$ of shell surface was removed using pre-ablation with $20 \times 150 \mu\text{m}$ laser spot to avoid any potential surface contamination. This pre-ablation significantly improved signal stability and eliminated spikes in Al, Mn, Fe, Zn, which were monitored for surface contamination commonly associated with cutting and polishing during sample preparation. The ICP-MS sensitivity was optimised using NIST612 reference glass material for maximum sensitivity across Li-U mass range and maintaining ThO/Th < 0.5% and Th/U ratio \sim 1. Data reduction involved initial screening of spectra for outliers, subtraction of the mean background intensities (measured with the laser turned off) from the analysed isotope intensities, internal standardisation to ⁴³Ca, and external standardisation using the NIST-SRM612 glass reference

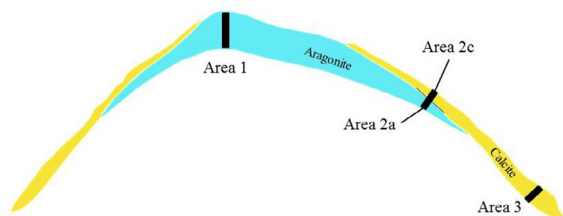


Fig. 1. Sketch of a transversal section of a shell indicating polymorph distribution and areas that were selected for LA-ICPMS (black bars).

material. In-house eBlue calcite and also NIST610 reference glass were used to monitor long term standards reproducibility.

Three areas of transversal shell sections were analysed (Fig. 1). Area 1 was comprised of aragonite, area 3 of calcite, and area 2 included an aragonitic as well as a calcitic part, which were analysed separately. Depending on the size of the area, ca. 100–500 individual laser-ablation profiles were carried out for each. Shell Me/Ca ratios are reported as the average values (\pm SE). The detection limit for U was ca. 5 nmol/mol.

Shell Me/Ca ratios are given in [mmol/mol]. With the exception of B (see explanation below), the partitioning coefficient K_{DMe} was calculated as follows: $K_{DMe} = (Me/Ca)_{cc}/(Me/Ca)_{sw}$, with $(Me/Ca)_{cc}$ = shell Me/Ca in [mol/mol] and $(Me/Ca)_{sw}$ = seawater Me/Ca in [mol/mol].

Since B does not substitute for Ca in the crystal lattice of calcium carbonates but for a CO_3 group (Hemming et al., 1995) the B partitioning coefficient K_{DB} was calculated according to: $K_{DB} = (B/Ca)_{cc}/(borate/bicarbonate)_{sw}$ with $(B/Ca)_{cc}$ = shell B/Ca in [mol/mol] and $(borate/bicarbonate)_{sw}$ = seawater borate/bicarbonate in [mol/mol]. All K_{DMe} values are reported as $K_{DMe} * 1000$.

2.4. Me/Ca ratios in seawater

The seawater sample was taken at the low pH site where the L-shells were sampled. The seawater was filtered (0.45 μ m Millipore cellulose acetate membrane filter) and stored in PE flacons (prewashed in ultra-pure Q grade de-ionised water) and then acidified to 1% with MERK Suprapur trace free HNO_3 . Ca and Mg concentrations were analysed through IC according to Gross et al. (2008). Li, B and Sr were analysed through ICPMS (Nollet and De Gelder, 2013) equipped with collision cell (Agilent 7500ce ORS technology) for interferences removal.

Element concentrations were quantified by averaging three duplicate analyses for each sample using external calibration. The analytical precision and accuracy for repeated analyses of the sea water samples, international and internal standards were better than 5%.

Seawater Me/Ca ratios at the sampling sites are assumed constant for the elements considered here. A variability of Me/Ca over time would require a substantial fresh water influx from a large river which would result in a variable salinity. In accordance with the absence of large rivers in the area, the salinity is constant (Frieder, 2013).

3. RESULTS

Transversal sections of *Patella caerulea* shells collected within (L-shells) and outside (N-shells) the Ischia CO_2 vent site were analysed for Sr/Ca, Mg/Ca, Li/Ca, B/Ca, and U/Ca by means of LA-ICPMS. We analysed two aragonitic and two calcitic areas (Fig. 1). U/Ca in all *P. caerulea* shells was below the detection limit of ca. 5 nmol/mol. The other Me/Ca ratios in N-shells are given in [mmol/mol] (standard error) in the following (Table S1). Sr/Ca in area 1 was 1.85 (0.16), in area 2a 1.79 (0.13), in area 3 1.64 (0.03), and in area 2c 1.65 (0.04). Mg/Ca in the area 1 was 0.63 (0.07), in area 2a 0.52 (0.05), in area 3 18.68 (1.34), and in area 2c 24.27 (4.02). Li/Ca in area 1 was 0.0052 (0.0003), in area 2a 0.0043 (0.0002), in area 3 0.0163 (0.0019), and in area 2c 0.0211 (0.0032). B/Ca in area 1 was 0.0107 (0.0020), in area 2a 0.0060 (0.0002), in area 3 0.0091 (0.0024), and in area 2c 0.0196 (0.0044).

Me/Ca ratios in L-shells are given in [mmol/mol] (standard error) in the following. Sr/Ca in the area 1 was 1.95 (0.04), in area 2a 1.95 (0.04), in area 3 1.62 (0.02), and in area 2c 1.74 (0.08). Mg/Ca in the area 1 was 0.77 (0.05), in area 2a 0.78 (0.14), in area 3 19.72 (1.68), and in area 2c 22.65 (1.49). Li/Ca in area 1 was 0.0036 (0.0001), in area 2a 0.0031 (0.0004), in area 3 0.0107 (0.0015), and in area 2c 0.0142 (0.0032). B/Ca in the area 1 was 0.0086 (0.0016), in area 2a 0.0055 (0.0003), in area 3 0.0075 (0.0013), and in area 2c 0.0124 (0.0022).

The seawater at the sampling site contained 0.0087 mol/mol Sr/Ca, 6.3490 mol/mol Mg/Ca, 0.0018 mol/mol Li/Ca, and 0.0425 mol/mol B/Ca. The seawater borate/bicarbonate ratio was 0.0385 mol/mol at the control site where the N-shells were sampled, and 0.0012 mol/mol at the vent site where the L-shells were sampled (Table S2).

We calculated the average partitioning coefficients K_{DMe} for aragonite and calcite separately using the respective Me/

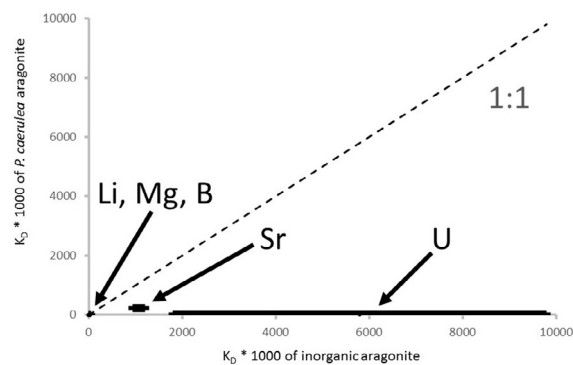


Fig. 2. Aragonite partitioning coefficients of Sr, Mg, Li, B, and U of *Patella caerulea* shells versus the respective partitioning coefficient of inorganic precipitates. Values for *P. caerulea* are from Table 1. Values for inorganic precipitates represent the published range for each element: Sr aragonite: Zhong and Mucci (1989), Gaetani and Cohen (2006), Mg aragonite: Gaetani and Cohen (2006), Li aragonite: Marriott et al. (2004), B aragonite: Mavromatis et al. (2015) based on borate/carbonate (Holcomb et al., 2016) based on borate/bicarbonate, U aragonite: Meece and Benninger (1993).

Ca ratios of seawater, with the exception of B, for which we used the borate/bicarbonate ratio of the control site. We report $K_{\text{DMe}} \cdot 1000$ (standard error) in the following. For aragonite the partitioning coefficients were Sr 216 (6), Mg 0.11 (0.01), Li 2.24 (0.13), B 0.20 (0.02). For calcite the partitioning coefficients were Sr 191 (3), Mg 3.36 (0.19), Li 8.61 (0.84), B 0.32 (0.05). Table S3 additionally shows K_{DMe} for L-shells and N-shells separately.

4. DISCUSSION

Although a number of studies addressed minor element (Me) partitioning in molluscs, these studies focus on particular aspects, such as temperature reconstruction (Schifano, 1984; Takesue and van Green, 2004; Freitas et al., 2005; Fenger et al., 2007; Ferguson et al., 2011; ; Schöne et al., 2011; Ullmann et al., 2013), effects of the seawater carbon system on B/Ca and U/Ca (McCoy et al., 2011; Hahn et al., 2012), and effects of growth rate on e.g., Sr/Ca (Gillikin et al., 2005; Lorrain et al., 2005; Carre et al., 2006; Sosdian et al., 2006; Thébault et al., 2009). Moreover, these studies used different species, which makes it difficult to relate the data to a single conceptual biomineralisation model. We therefore analysed the partitioning of various elements into both aragonitic and calcitic shell parts of *Patella caerulea*, collected from both outside and inside an Ischia CO₂ vent side. Three of these elements do not show a seawater carbon chemistry dependent speciation (Sr, Mg, and Li), while the other two do (U and B, McClaine et al., 1955; Dickson, 1990). The most fundamental question to ask when thinking about conceptual biomineralisation that can explain element partitioning is: “Can the partitioning behaviour of various elements be explained in terms of inorganic precipitation from a known parent solution, here seawater?” This aspect is of fundamental importance in the case of marine molluscs.

In marine molluscs the extrapallial fluid (EPF) is an aqueous solution similar to seawater in ionic composition, but containing additional proteins and polysaccharides, and possibly a carbon chemistry which is different from that of the surrounding seawater (Crenshaw, 1972; Misogianes and Chasteen, 1979; Coimbra et al., 1988; Heinemann et al., 2012; Marin et al., 2012). The initial idea was that calcium carbonate is precipitated in the extrapallial space, with direct contact between the mineral phase and the EPF, making the extrapallial fluid the parent solution from which the calcium carbonate shell is precipitated (Crenshaw, 1972; Misogianes and Chasteen, 1979). The similarity in ionic composition between the EPF and seawater makes element partitioning an ideal testing ground for this biomineralisation scenario. If this “EPF scenario” is operative, element partitioning should be explicable in terms of inorganic precipitation from seawater.

4.1. The partitioning coefficient

First, we look at the partitioning coefficient K_{D} . Typical seawater features a U concentration of ca. 13 nM and a U/Ca ratio of ca. $1.3 \cdot 10^{-6}$ mol/mol (Ku et al., 1977; Shen and Dunbar, 1995). The lowest U partitioning coefficient

(K_{DU}) for calcite reported in the literature is 0.046 (Meece and Benninger, 1993). Based on these data, calcite, precipitated from solutions that show a chemical composition similar to seawater, should therefore contain >60 nmol/mol U/Ca. *Patella caerulea* calcite by contrast contains <5 nmol/mol U/Ca (see also Material and Methods). Inorganic aragonite has a minimal K_{DU} of 2 and should contain a minimum of ca. 2600 nmol/mol U/Ca (Meece and Benninger, 1993). *P. caerulea* aragonite by contrast contains <5 nmol/mol U/Ca. Based on these data, we conclude that *P. caerulea*, in contrast to corals and sclerosponges (Swart and Hubbard, 1982; Rosenheim et al., 2005), discriminates strongly against U.

The B partitioning coefficient K_{DB} of *P. caerulea* calcite is by one order of magnitude lower than the one reported for inorganic calcite (Table 1, He et al., 2013). The same is possibly true for *P. caerulea* aragonite, although there remains uncertainty as to the full range of inorganic values (Table 1, Holcomb et al., 2016).

The Mg partitioning coefficients K_{DMg} for both aragonite and calcite do not resemble the respective inorganic ones (Table 1, Mucci and Morse, 1983; Zhong and Mucci, 1989; Gaetani and Cohen, 2006). The same is true for Sr with the exception of the calcite K_{DSr} , which falls within the range of inorganic values (Table 1, Lorens, 1981; Mucci and Morse, 1983; Zhong and Mucci, 1989; Tesoriero and Pankow, 1996; Gaetani and Cohen, 2006; Tang et al. 2008).

The Li partitioning coefficient K_{DLi} of both aragonite and calcite is indistinguishable from inorganic values (Table 1, Okumura and Kitano, 1986; Marriott et al., 2004).

Whereas our seawater Sr/Ca and B/Ca are very close to average seawater values, Li/Ca is by a factor of 1.35 too low and Mg/Ca is by a factor of 1.23 too high (Table S2, Broecker and Peng, 1982). Since we measured Me/Ca of seawater only at the vent site, it is possible that the unusual Li and Mg values are caused by the seep and are therefore not applicable to the control site. However, even when the N-shell K_{D} values for Li and Mg are corrected by the above mentioned factors, our conclusions remain unchanged.

On the whole, the partitioning coefficients of the elements analysed here are different from the ones of inorganically precipitated aragonite and calcite (Figs. 2, 3). This points to a biologically modified element partitioning. It should be mentioned that partitioning coefficients of inorganically precipitated aragonite and calcite comprise a thermodynamic value (strongest fractionation) and a range of values influenced by precipitation kinetics (e. g. Lorens, 1981). For some elements such as Sr, Mg, and probably U the possible range of partitioning coefficients is well known, for other elements such as B and possibly Li, there remains some uncertainty. However, this uncertainty does not affect our conclusion, because the latter is based on all analysed elements. Please note that considering e. g. Li, or Sr in calcite alone would have led to the contrary conclusion.

This is also illustrated by previous studies showing that element partitioning into marine biogenic carbonates differs from that predicted on the basis of inorganic precipitation

Table 1

Minor elements (Me) partitioning behaviour of *Patella caerulea* in comparison to its inorganic counterpart. We show the partitioning coefficient, the differential partitioning into aragonite and calcite, the effect of calcification/precipitation rate, and the effect of seawater carbonate chemistry. A > C means that the respective partitioning coefficient is higher in aragonite than in calcite.

	K _D * 1000 (S.E.)				Polymorph, A = aragonite, C = calcite		Rate	C-chemistry, N = control site, L = low pH site			
	<i>Patella</i> average		Inorganic		<i>Patella</i>	Inorganic	<i>Patella</i>	Inorganic	<i>Patella</i>	Inorganic	
	Aragonite	Calcite	Aragonite	Calcite							
Sr	216 (6)	191 (3)	940–1200	20–300	A > C	A > C	Constant	Up	n/a	n/a	
Mg	0.11 (0.01)	3.36 (0.19)	1–2	15–30	C > A	C > A	Aragonite up/calcite constant	Up	Aragonite L > N/calcite constant	Constant	
Li	2.24 (0.13)	8.61 (0.84)	3–4	2–9	C > A	A = C	Down	Up	n/a	n/a	
B based on borate/ bicarbonate	0.20 (0.02)	0.32 (0.05)	0.3–52	1.27–2.13	C > A	A > C ^a	n/a	n/a	L > N	Constant	
B based on borate/carbonate	0.02 (0.002)	0.03 (0.004)	3 * 10 ⁻³ to 3 *	3 * 10 ⁻⁴ to 3 *	C > A	A > C	n/a	n/a	Constant	Constant	
U	Max 3.8	Max 3.8	1800–9800	46–420	n/a	n/a	n/a	n/a	n/a	n/a	

n/a = not applicable.

^a Please note that K_{DB} is higher in aragonite than in calcite even when calculated based on borate/bicarbonate. This is concluded from experiments where both aragonite and calcite were precipitated under comparable conditions. K_D values of inorganic precipitates were taken from: Sr aragonite: [Zhong and Mucci \(1989\)](#), [Gaetani and Cohen \(2006\)](#), Mg aragonite: [Gaetani and Cohen \(2006\)](#), Li aragonite: [Marriott et al. \(2004\)](#), B aragonite: [Mavromatis et al. \(2015\)](#) based on borate/carbonate ([Holcomb et al. 2016](#) based on borate/bicarbonate), U aragonite: [Meece and Benninger \(1993\)](#), Sr calcite: [Mucci and Morse \(1983\)](#), [Lorens \(1981\)](#), [Tesoriero and Pankow \(1996\)](#), [Tang et al. \(2008\)](#), Mg calcite: [Mucci and Morse \(1983\)](#), [Zhong and Mucci \(1989\)](#), Li calcite: [Okumura and Kitano \(1986\)](#), [Marriott et al. \(2004\)](#), B calcite: [Mavromatis et al. \(2015\)](#) based on borate/carbonate (1.27–2.13 * 10⁻³, [He et al. \(2013\)](#), based on borate/bicarbonate), U calcite: [Meece and Benninger \(1993\)](#). Rate effects on inorganic K_D were taken from [Lorens \(1981\)](#), [Busenberg and Plummer \(1985\)](#), [Gabitov et al. \(2014\)](#), [Uchikawa et al. \(2015\)](#). Carbon chemistry effects on inorganic K_D were taken from [Hemming et al. \(1995\)](#), [Hartley and Mucci \(1996\)](#).

Table 2

Conclusions drawn from the data in Table 1. The question answered in each case is “Is this Me partitioning behaviour possible in the EPF-scenario?”.

Minor element	Can the EPF be the parent solution for shell calcium carbonate? Y = Yes, N = No			
	K _D	Polymorph	Rate	C-chemistry
Sr	N	Y	N	Y
Mg	N	Y	N	Y
Li	Y	N	N	Y
B	N	N	n/a	Y
U	N	n/a	n/a	Y

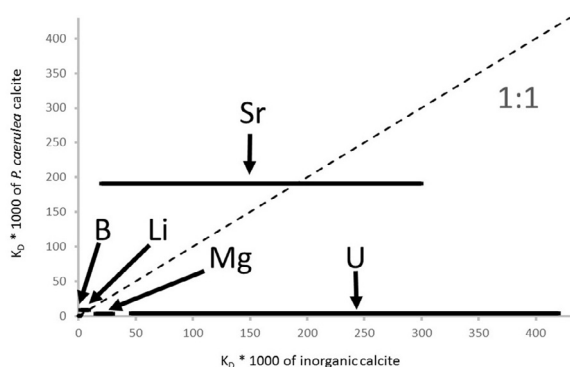


Fig. 3. Calcite partitioning coefficients of Sr, Mg, Li, B, and U of *Patella caerulea* shells versus the respective partitioning coefficient of inorganic precipitates. Values for *P. caerulea* are from Table 1. Values for inorganic precipitates represent the published range for each element: Sr calcite: Mucci and Morse (1983), Lorens (1981), Tesoriero and Pankow (1996), Tang et al. (2008), Mg calcite: Mucci and Morse (1983), Zhong and Mucci (1989), Li calcite: Okumura and Kitano (1986), Marriott et al. (2004), B calcite: Mavromatis et al. (2015) based on borate/carbonate ($1.27\text{--}2.13 \times 10^{-3}$, He et al. (2013), based on borate/bicarbonate), U calcite: Meece and Benninger (1993).

experiments. The latter is the case for Sr/Ca and Mg/Ca in aragonitic bivalves, and the aragonite of the gastropod *Conus*, for which a biological influence on element fractionation was suggested (Zhong and Mucci, 1989; Gillikin et al., 2005; Gaetani and Cohen, 2006; Carre et al., 2006; Sosdian et al., 2006). In the calcite of the fan mussel *Pinna*, Mg/Ca is lower than that of inorganic calcite, but Sr/Ca falls within the range of values reported for inorganic calcite (Lorens, 1981; Mucci and Morse, 1983; Freitas et al., 2005).

However, the absolute value of the partitioning coefficient is not the only aspect of an element's partitioning behaviour. In many cases, partitioning of elements is polymorph dependent and therefore differs for aragonite and calcite. This is the case for Sr, Mg, B, U, and maybe Li (Kitano et al., 1978; Lorens, 1981; Mucci and Morse, 1983; Okumura and Kitano, 1986; Zhong and Mucci, 1989; Meece and Benninger, 1993; Hemming et al., 1995; Tesoriero and Pankow, 1996; Marriott et al., 2004; Gaetani and Cohen, 2006; Tang et al., 2008). It is to this

differential partitioning into aragonite and calcite we now turn.

4.2. Differential partitioning into aragonite and calcite

Differential partitioning into aragonite and calcite (partitioning into aragonite relative to partitioning into calcite) is similar in N-shells and L-shells, showing that the difference in seawater carbon chemistry that characterizes the two sites did not change the general pattern observed. The same holds for the calcification rate, which was different for specimens from the two sites (Rodolfo-Metalpa et al., 2011). In *P. caerulea* shells Sr/Ca is by a factor of 1.1 higher in aragonite than in calcite. Given identical parent solution Sr/Ca, inorganic precipitates also display higher Sr/Ca in aragonite, although aragonite and calcite differ by a factor of 4–60 here (Table 1). Hence the trends in polymorph specific Sr partitioning (higher values in aragonite compared to calcite) are the same in *P. caerulea* shells and inorganic precipitates, but the numerical difference is not. The fact that inorganic precipitates show a more pronounced difference between aragonite and calcite in Sr/Ca might point to a non-inorganic Sr/Ca partitioning in *P. caerulea*. However, since the trends are the same, i.e. higher aragonite Sr/Ca in both *P. caerulea* and inorganic precipitates, the conservative conclusion is that the Sr partitioning of *P. caerulea* in this particular respect resembles the trend observed for inorganic precipitates. The Mg/Ca ratio is higher in calcite compared to aragonite in both *P. caerulea* and inorganic precipitates (Tables 1, 2, and S1, Fig. 4). Hence, the polymorph specific partitioning of Mg also is indistinguishable from the inorganic system. However, the polymorph specific partitioning of Li and B in *P. caerulea* differs from the inorganic system. The Li/Ca ratio is higher in *P. caerulea* calcite, whereas there is no difference in inorganic precipitates (Tables 1, S1, Fig. 4). The B/Ca ratio also is higher in *P. caerulea* calcite, while it is lower in inorganic calcite (Tables 1, S1, Fig. 4). Therefore, the polymorph specific partitioning of Li and B in *P. caerulea* is not explainable in terms of inorganic precipitation (Tables 1 and 2).

4.3. The influence of seawater carbon chemistry (and calcification rate)

The B/Ca proxy for seawater carbon chemistry in foraminifera relies on the sole incorporation of borate into calcium carbonate, which is assumed to compete with bicarbonate, not with Ca (Hemming et al., 1995; Allen et al., 2012; Kaczmarek et al., 2015). Therefore a linear positive correlation between B/Ca in calcium carbonate and borate/bicarbonate in seawater is expected. Since the seawater borate/bicarbonate ratio is by a factor of ca. 33 higher at the control site (N-shells, see Results), it is to be expected that B/Ca will be higher in N-shells precisely by that factor. This, however, is not the case. In aragonite there is no difference at all (Table S1), and in calcite there is a small difference (factor of 1.6) in area 2 only (Table S1). That means that B/Ca is not influenced by seawater carbon chemistry. This shows that unmodified seawater is not the parent solution for *P. caerulea* shell calcium

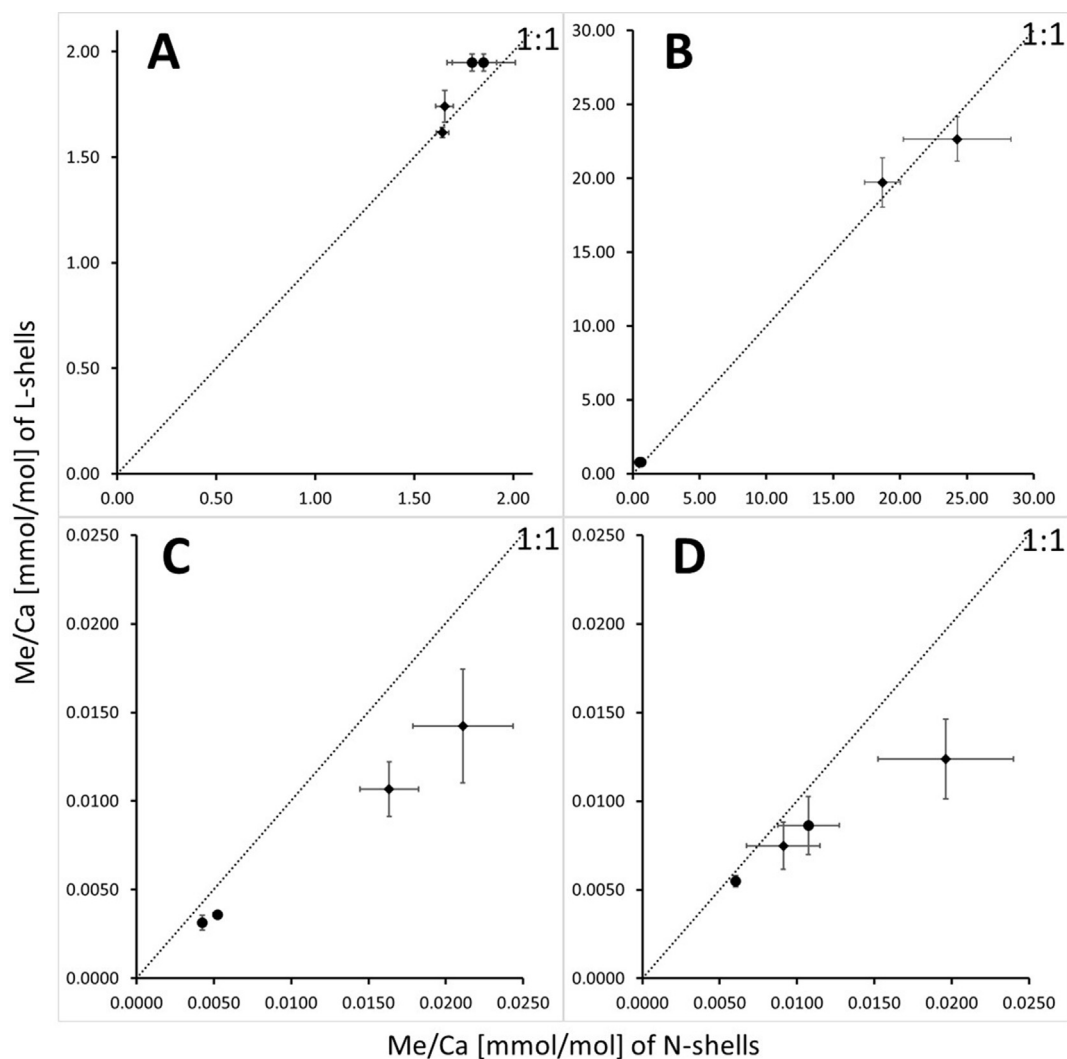


Fig. 4. Me/Ca of L-shells versus Me/Ca of N-shells. (A) Sr/Ca, (B) Mg/Ca, (C) Li/Ca, (D) B/Ca. Each data point represents the average Me/Ca of each area (see Fig. 1). Circles represent aragonite and diamonds represent calcite.

carbonate. However, the parent solution could be modified seawater; modified with respect to carbon chemistry only. This is in agreement with a study by Heinemann et al. (2012) which suggests molluscs might control the carbon chemistry in the EPF.

Patella Mg/Ca in aragonite and Li/Ca in both aragonite and calcite are affected by seawater carbon chemistry (Tables 1, and S1, Fig. 4). Carbon chemistry effects on the partitioning of elements other than U and B are often more difficult to explain because many elements do not show a pronounced speciation change with variable carbon chemistry. Therefore indirect effects have been proposed e.g. in foraminifera. Carbon chemistry related changes in Sr/Ca, Mg/Ca, and Li/Ca of foraminiferal tests are supposed to be due to calcification rate changes (Russell et al., 2004; Hall and Chan, 2004; Dissard et al., 2010; Yu et al., 2014). The argument is that higher pH and carbonate ion concentration lead to higher calcification rate, which in

turn alters the partitioning coefficients. Since calcification rate in *P. caerulea* from within the Ischia CO₂ vent site (L-shells) is higher than in specimens from outside (N-shells) (Rodolfo-Metalpa et al., 2011), it might be expected that Sr/Ca, Mg/Ca, and Li/Ca also are. In several molluscs positive correlations between partitioning coefficients and growth rate were reported (Gillikin et al., 2005; Lorrain et al., 2005; Carre et al., 2006; Sosdian et al., 2006; Thébaud et al. 2009). The opposite is the case for Li/Ca (Tables 1 and S1). Sr/Ca does not change in response to changes in calcification rate (Tables 1 and S1). Only Mg/Ca is, at least in aragonite, indeed higher in L-shells (Tables 1 and S1). This shows that carbon chemistry-induced calcification rate changes do not control Me partitioning.

We evaluated the partitioning behaviour of several elements in *P. caerulea* with respect to their similarity to the inorganic system. In many cases we found differences. A significant difference between values expected based on

inorganic processes and actually measured values are well documented for most biogenic carbonates, and the term “vital effects” is used to describe this observation. Vital effects are thought to be caused by a number of physiological processes involved in the ion transport from seawater to the site of calcification. Since in the EPF scenario a direct precipitation out of the EPF is assumed, three out of the four aspects considered here, would predict values that are expected for inorganic systems (no physiological processes causing “vital effects” involved). These aspects are growth rate dependence, polymorph dependence, and the absolute value of the partitioning coefficient. The objective of our study was to find out whether this prediction holds true. The unambiguous answer is no. There are “vital effects” in the absolute values of the distribution coefficients of Sr, Mg, B, and U, in the polymorph dependence of Li and B, and in the rate dependence of Sr, Mg, and Li (Tables 1 and 2). Hence, our data are incompatible with the EPF scenario.

As mentioned in the Introduction, the EPF scenario is not the only biomineralisation model discussed for molluscs. In recent years an alternative hypothesis (hereafter termed the mantle-scenario), which features a sub-space within the extrapallial space has been proposed. In the mantle-scenario there is a close connection of the outer mantle epithelium and the mineral surface during calcium carbonate precipitation (Simkiss and Wilbur, 1989; Beniash et al., 1999; Addadi et al., 2006; Suzuki et al., 2009; Cuif et al., 2011). Most recently, Planchon et al. (2013) described that as a “self-contained space located close to calcification sites” which separates the EPF from the mineral surface. The small space between the outer mantle epithelium and the mineral surface is filled with a protein gel excreted by the epithelium cells, which also transport ions such as Ca into this space (see references above). As a result, the environment in which calcium carbonate precipitates differs from the EPF in two important ways. Firstly, it is not an aqueous solution, but a protein gel. Secondly, the minor element to calcium ratios (Me/Ca) will not resemble those of the EPF, i.e. those of seawater (the transport of ions from the EPF into this “self-contained space” will most likely lead to an elemental and isotopic fractionation as it is likely mediated by transmembrane transport via ion pumps or channels). In the following we will revisit the four characteristic “features” of element partitioning discussed above in their relation to the two biomineralisation models, i.e., the EPF and the mantle scenario.

Feature one, “distribution coefficient”: Since the EPF-scenario suggests a direct shell precipitation from the EPF (seawater-like ionic composition, Crenshaw, 1972; Misogianes and Chasteen, 1979; Coimbra et al., 1988; Heinemann et al., 2012), Me distribution coefficients should be close to the ones of inorganically precipitated calcite and aragonite. Cell physiological processes involved in the formation of biogenic minerals, such as transmembrane ion transport, often lead to Me fractionation producing distribution coefficients that may be different from those determined for inorganic precipitation. The mantle-scenario does not allow predicting any values for the distribution coefficient since the impact of cell physiological processes is unknown.

Feature two “polymorph dependence”: Distribution coefficients are strongly polymorph dependent. If aragonite and calcite are inorganically precipitated from the same parent solution their distribution coefficients are different due to their difference in crystal structure. For the EPF-scenario this would mean that the precipitation of aragonite and calcite from the same EPF should result in different distribution coefficients for the different polymorphs (Watabe and Wilbur, 1960; Kitano et al., 1978; Lorens, 1981; Mucci and Morse, 1983; Okumura and Kitano, 1986; Zhong and Mucci, 1989; Meece and Benninger, 1993; Hemming et al., 1995; Belcher et al., 1996; Falini et al., 1996; Tesoriero and Pankow, 1996; Marriott et al., 2004; Gaetani and Cohen, 2006; Tang et al., 2008). Again, for the mantle-scenario a prediction is not possible since the impact of cell physiology cannot be predicted.

Feature three “growth rate”: The precipitation rate of calcium carbonate from an aqueous solution significantly influences the incorporation of Me^{2+} and boron (Kaczmarek et al., 2016). Rodolfo-Metalpa (2011) showed that limpets from low pH areas of the Ischia CO_2 vents calcified faster than those growing under normal pH. They considered this an adaptation to cope with dissolution caused by acidified seawater since the limpets could not “switch off” this hypercalcification when transplanted away from the high CO_2 conditions. Since the growth rate of *P. caerulea* shells is faster inside the CO_2 vent site (Rodolfo-Metalpa et al., 2011) it can be assumed that the distribution coefficients should be different for specimens collected at the two sites. This assumption is only true for the EPF-scenario because we do not know whether the relationship between growth rate and K_D holds in the mantle-scenario. See also Lorens, 1981; Busenberg and Plummer, 1985; Russell et al., 2004; Hall and Chan, 2004; Gillikin et al., 2005; Lorrain et al., 2005; Carre et al., 2006; Langer et al., 2006; Sossdian et al., 2006; Thébault et al. 2009; Gabitov et al., 2014; Yu et al., 2014; Uchikawa et al., 2015.

Feature four “carbon chemistry”: The carbonate chemistry of seawater is characterized by the interlinked parameters bicarbonate, carbonate ion, and CO_2 concentration, alkalinity, the total dissolved inorganic carbon, and pH. The values of some of these parameters are reflected in the elemental and isotopic composition of the precipitated calcium carbonate. There is a well-known correlation between pH and the boron isotopic composition of calcium carbonate (Hemming and Hanson, 1992; Hemming et al., 1995) and a correlation between U/Ca and CO_3^{2-} and between B/Ca and CO_3^{2-} or HCO_3^- (Russell et al., 2004; Yu et al., 2007; Keul et al., 2013; Kaczmarek et al., 2015; Howes et al., 2017). Due to the difference in carbonate chemistry inside and outside the CO_2 vent site it can be assumed that this difference is reflected in B/Ca and U/Ca content of the shells. Although a correlation between shell B/Ca and U/Ca respectively and seawater carbonate chemistry has been shown for some organisms such as foraminifera (e.g. Keul et al., 2013; Kaczmarek et al., 2015; Howes et al., 2017), other organisms such as molluscs showed ambiguous data (e.g. McCoy et al., 2011). This inconclusive finding is most likely related to the fact that molluscs regulate the pH inside the EPF (Crenshaw, 1972; Misogianes

and Chasteen, 1979; Coimbra et al., 1988; Heinemann et al., 2012; Marin et al., 2012). Due to this complication in the interpretation of B/Ca and U/Ca values we do not regard them as suitable to differentiate between the mantle- and EPF-scenario. See also McClaine et al., 1955; Dickson, 1990; Hartley and Mucci, 1996; Russell et al., 2004; McCoy et al., 2011; Allen et al., 2012; Kaczmarek et al., 2015.

To conclude, all our data are compatible with the mantle-scenario, because the latter in general allows for vital effects. However, the mantle-scenario does not predict specific vital effects or minor elements, which should show vital effects. Therefore, it is important to look at various minor elements and different aspects of their partitioning behaviour. To the best of our knowledge, this is the first study that systematically undertakes such a multi-element, multi-aspect approach. Based on our dataset we conclude that the mantle hypothesis is superior to the EPF hypothesis. Moreover, our dataset will be helpful in the future, because its compatibility with every new rival biomineralisation model can be tested.

ACKNOWLEDGEMENTS

This work was supported by the Natural Environment Research Council (NE/N011708/1) and European Research Council (ERC) (grant 2010-NEWLOG ADG-267931 to H.E.).

APPENDIX A. SUPPLEMENTARY MATERIAL

Supplementary data associated with this article can be found, in the online version, at <https://doi.org/10.1016/j.gca.2018.02.044>.

REFERENCES

- Addadi L., Joester D., Nudelman F. and Weiner S. (2006) Mollusk shell formation: a source of new concepts for understanding biomineralization processes. *Chem. – Eur. J.* **12**, 981–987.
- Allen K. A., Hönisch B., Eggins S. M. and Rosenthal Y. (2012) Environmental controls on B/Ca in calcite tests of the tropical planktic foraminifer species *Globigerinoides ruber* and *Globigerinoides sacculifer*. *Earth Planet. Sci. Lett.* **351–352**, 270–280.
- Belcher A. M., Wu X. H., Christensen R. J., Hansma P. K., Stucky G. D. and Morse D. E. (1996) Control of crystal phase switching and orientation by soluble mollusc-shell proteins. *Nature* **381**, 56–58.
- Beniash E., Addadi L. and Weiner S. (1999) Cellular control over spicule formation in sea urchin embryos: a structural approach. *J. Struct. Biol.* **125**, 50–62.
- Bentov Shmue, Brownlee Coli and Erez Jonatha (2009) The role of seawater endocytosis in the biomineralization process in calcareous foraminifera. *PNAS* **106**, 21500–21504.
- Bowerbank J. S. (1844) On the structure of the shells of molluscan and conchyferous animals. *Trans. Microsc. Soc. London* **1**, 123–152.
- Broecker W. S. and Peng T. H. (1982) *Tracers in the Sea*. Eldigio Press, New York, pp. 1–690.
- Busenberg E. and Plummer L. N. (1985) Kinetic and thermodynamic factors controlling the distribution of SO_3^{2-} and Na^+ in calcites and selected aragonites. *Geochim. Cosmochim. Acta* **49**, 713–725.
- Carre M., Bentaleb I., Bruguier O., Ordinola E., Barrett N. T. and Fontugne M. (2006) Calcification rate influence on trace element concentrations in aragonitic bivalve shells: evidences and mechanisms. *Geochim. Cosmochim. Acta* **70**, 4906–4920.
- Coimbra J., Machado J., Fernandes P. L., Ferreira H. G. and Ferreira K. G. (1988) Electrophysiology of the mantle of *Anodonta cygnea*. *J. Exp. Biol.* **140**, 65–88.
- Crenshaw M. A. (1972) The inorganic composition of molluscan extrapallial fluid. *Biol. Bull.* **143**, 506–512.
- Cuif J.-P., Dauphin Y. and Sorauf J. E. (2011) *Biomaterials and Fossils Through Time*. Cambridge University Press, Cambridge, p. 490.
- Dickson A. G. (1990) Thermodynamics of the dissociation of boric acid in synthetic seawater from 273.15 to 318.15 K. *Deep-Sea Res.* **37**, 755–766.
- Dissard D., Nehrke G., Reichart G. J. and Bijma J. (2010) Impact of seawater pCO₂ on calcification and Mg/Ca and Sr/Ca ratios in benthic foraminifera calcite: results from culturing experiments with *Ammonia tepida*. *Biogeosciences* **7**, 81–93.
- Elderfield H., Cooper M. and Ganssen G. (2000) Sr/Ca in multiple species of planktonic foraminifera: implications for reconstructions of seawater Sr/Ca. *Geochem. Geophys. Geosyst.* **1**, 1017. <https://doi.org/10.1029/1999GC000031>.
- Erez J. (2003) The source of ions for biomineralization in foraminifera and their implications for paleoceanographic proxies. *Rev. Mineral Geochem.* **54**, 115–149.
- Erez J. and Braun A. (2007) Calcification in hermatypic corals is based on direct seawater supply to the biomineralization site. *Geochim. Cosmochim. Acta* **71**(15 Suppl 1), A260.
- Falini G., Albeck S., Weiner S. and Addadi L. (1996) Control of aragonite or calcite polymorphism by mollusk shell macromolecules. *Science* **271**, 67–69.
- Fenger T., Surge D., Schöne B. and Milner N. (2007) Sclerochronology and geochemical variation in limpet shells (*Patella vulgata*): a new archive to reconstruct coastal sea surface temperature. *Geochem. Geophys. Geosyst.* **8**, Q07001. <https://doi.org/10.1029/2006GC001488>.
- Ferguson J. E., Henderson G. M., Fab D. A., Finlayson J. C. and Charnley N. R. (2011) Increased seasonality in the Western Mediterranean during the last glacial from limpet shell geochemistry. *Earth Planet. Sci. Lett.* **308**, 325–333.
- Foster, G.L., 2008b. Seawater pH, pCO₂ and [CO₃²⁻] variations in the Caribbean Sea over the last 130 kyr: A boron isotope and B/Ca study of planktic foraminifera EPSL 271, pp. 254–266. doi: 10.1016/j.epsl.2008.04.015.
- Freitas P., Clarke L. J., Kennedy H., Richardson C. and Abrantes F. (2005) Mg/Ca, Sr/Ca, and stable-isotope ($\delta^{18}\text{O}$ and $\delta^{13}\text{C}$) ratio profiles from the fan mussel *Pinna nobilis*: seasonal records and temperature relationships. *Geochem. Geophys. Geosyst.* **6**, Q04D14. <https://doi.org/10.1029/2004GC000872>.
- Frieder C. A. (2013) *Evaluating Low Oxygen and pH Variation and its Effects on Invertebrate Early Life Stages on Upwelling Margins*. University of California, San Diego, PhD Thesis, <https://escholarship.org/uc/item/74m0h54p>.
- Gabitov R. I., Sadekov A. and Leinweber A. (2014) Crystal growth rate effect on Mg/Ca and Sr/Ca partitioning between calcite and fluid: an in situ approach. *Chem. Geol.* **367**, 70–82.
- Gaetani G. A. and Cohen A. L. (2006) Element partitioning during precipitation of aragonite from seawater: a framework for understanding paleoproxies. *Geochim. Cosmochim. Acta* **70**, 4617–4634.

- Gagnon Alexander C., Adkins Jess F. and Erez Jonatha (2012) Seawater transport during coral biomineralization. *Earth Planet. Sci. Lett.* **329–330**, 150–161.
- Gillikin D. P., Lorrain A., Navez J., Taylor J. W., André L., Keppens E., Baeyens W. and Dehairs F. (2005) Strong biological controls on Sr/Ca ratios in aragonitic marine bivalve shells. *Geochem. Geophys. Geosyst.* **6**, Q05009. <https://doi.org/10.1029/2004GC000874>.
- Gros N., Camoes M. F., Oliveira C. and Silva M. C. R. (2008) Ionic composition of seawaters and derived saline solutions determined by ion chromatography and its relation to other water quality parameters. *J. Chromatogr. A* **1210**, 92–98.
- Hahn S., Rodolfo-Metalpa R., Griesshaber E., Schmahl W. W., Buhl D., Hall-Spencer J. M., Baggini C., Fehr K. T. and Immenhauser A. (2012) Marine bivalve shell geochemistry and ultrastructure from modern low pH environments: environmental effect versus experimental bias. *Biogeosciences* **9**, 1897–1914.
- Hall J. M. and Chan L.-H. (2004) Li/Ca in multiple species of benthic and planktonic foraminifera: thermocline, latitudinal, and glacial-interglacial variation. *Geochim. Cosmochim. Acta* **68**, 529–545.
- Hall-Spencer J. M., Rodolfo-Metalpa R., Martin S., Ransome E., Fine M., Turner S. M., Rowley S. J., Tedesco D. and Buia M.-C. (2008) Volcanic carbon dioxide vents show ecosystem effects of ocean acidification. *Nature* **454**(7200), 96–99.
- Hartley G. and Mucci A. (1996) The influence of PCO₂ on the partitioning of magnesium in calcite overgrowths precipitated from artificial seawater at 25 °C and 1 atm total pressure. *Geochim. Cosmochim. Acta* **60**, 315–324.
- He M. Y., Xiao Y. K., Jin Z. D., Liu W. G., Ma Y. Q., Zhang Y. L. and Luo C. G. (2013) Quantification of boron incorporation into synthetic calcite under controlled pH and temperature conditions using a differential solubility technique. *Chem. Geol.* **337**, 67–74.
- Hedegaard C., Lindberg D. R. and Bandel K. (1997) Shell microstructure of a Triassic patellogastropod limpet. *Lethaia* **30**, 331–335.
- Heinemann A., Fietzke J., Melzner F., Böhm F., Thomsen J., Garbe-Schönberg D. and Eisenhauer A. (2012) Conditions of *Mytilus edulis* extracellular body fluids and shell composition in a pH-treatment experiment: acid-base status, trace elements and $\delta^{11}\text{B}$. *Geochem. Geophys. Geosyst.* **13**, Q01005. <https://doi.org/10.1029/2011GC003790>.
- Hemming N. G. and Hanson G. N. (1992) Boron isotopic composition and concentration in modern marine carbonates. *Geochim. Cosmochim. Acta* **56**(1), 537–543.
- Hemming N. G., Reeder R. J. and Hanson G. N. (1995) Mineral-fluid partitioning and isotopic fractionation of boron in synthetic calcium carbonate. *Geochim. Cosmochim. Acta* **59**, 371–379.
- Holcomb M., DeCarlo T. M., Gaetani G. A. and McCulloch M. (2016) Factors affecting B/Ca ratios in synthetic aragonite. *Chem. Geol.* **437**, 67–76.
- Hönisch B., Hemming N. G., Grottoli A. G., Amat A., Hanson G. N. and Bijma J. (2004) Assessing scleractinian corals as recorders for paleo-pH: empirical calibration and vital effects. *Geochim. Cosmochim. Acta* **68**(18), 3675–3685.
- Howes E. L., Kaczmarek K., Raitzsch M., Mewes A., Bijma N., Horn I., Misra S., Gattuso J. P. and Bijma J. (2017) Decoupled carbonate chemistry controls on the incorporation of boron into *Orbulina universa*. *Biogeosciences* **14**, 415–430.
- Kaczmarek K., Langer G., Nehrke G., Horn I., Misra S., Janse M. and Bijma J. (2015) Boron incorporation in the foraminifer *Amphistegina lessonii* under a decoupled carbonate chemistry. *Biogeosciences* **12**, 1753–1763.
- Kaczmarek K., Nehrke G., Misra S., Bijma J. and Elderfield H. (2016) Investigating the effects of growth rate and temperature on the B/Ca ratio and $\delta^{11}\text{B}$ during inorganic calcite formation. *Chem. Geol.* **421**, 81–92.
- Keul N., Langer G., de Nooijer L. J., Nehrke G., Reichart G.-J. and Bijma J. (2013) Incorporation of uranium in benthic foraminiferal calcite reflects seawater carbonate ion concentration. *Geochem. Geophys. Geosyst.* **14**, 102–111.
- Kitano Y., Okumura M. and Idogaki M. (1978) Coprecipitation of borate-boron with calcium carbonate. *Geochem. J.* **12**, 183–189.
- Ku T.-L., Knauss K. G. and Mathieu G. G. (1977) Uranium in open ocean: concentration and isotopic composition. *Deep Sea Res.* **24**, 1005–1017.
- Lea, D.W., 2014. Elemental and isotopic proxies of past ocean temperatures. In: Holland, H.D., Turekian, K.K., (Eds.) Treatise on Geochemistry, second ed., vol. 8, Elsevier, Oxford, pp. 373–397.
- Langer G., Gussone N., Nehrke G., Riebesell U., Eisenhauer A., Kuhnert H., Rost B., Trimborn S. and Thoms S. (2006) Coccolith strontium to calcium ratios in *Emiliania huxleyi*: the dependence on seawater strontium and calcium concentrations. *Limnol. Oceanogr.* **51**, 310–320.
- Langer G., Nehrke G., Baggini C., Rodolfo-Metalpa R., Hall-Spencer J. M. and Bijma J. (2014) Limpets counteract ocean acidification induced shell corrosion by thickening of aragonitic shell layers. *Biogeosciences* **11**, 7363–7368.
- Linnaeus, C. (1758). *Systema Naturae per regna tria naturae, secundum classes, ordines, genera, species, cum characteribus, differentiis, synonymis, locis*. Editio decima, reformata. Laurentius Salvius: Holmiae. ii, 824 pp.
- Lorrain A., Gillikin D. P., Paulet Y.-M., Chauvaud L., Le Mercier A., Navez J. and André L. (2005) Strong kinetic effects on Sr/Ca ratios in the calcitic bivalve *Pecten maximus*. *Geology* **33**, 965–968.
- Lorens R. B. (1981) Sr, Cd, Mn and Co distribution coefficients in calcite as a function of calcite precipitation rate. *Geochim. Cosmochim. Acta* **45**, 553–561.
- Marin F., Le Roy N. and Marie B. (2012) The formation and mineralization of mollusk shell. *Front. Biosci. (Schol. Ed.)* **1**(4), 1099–1125.
- Marriott C. S., Henderson G. M., Crompton R., Staubwasser M. and Shaw S. (2004) Effect of mineralogy, salinity, and temperature on Li/Ca and Li isotope composition of calcium carbonate. *Chem. Geol.* **212**, 5–15.
- Mass, Tali, Giuffre, Anthony J., Sun, Chang-Yu, Stiffler, Cayla A., Frazier, Matthew J., Neder, Maayan, Tamura, Nobumichi, Stan, Camelia V., Marcus, Matthew A., Gilbert, Pupa U.P.A., 2017. Proceedings of the National Academy of Sciences of the United States of America, vol. 114, no. 37, pp. E7670–E7678.
- Mavromatis Vasileio, Montouillout Valéri, Noireaux Johann, Gaillardet Jérôm and Schott Jacques (2015) Characterization of boron incorporation and speciation in calcite and aragonite from co-precipitation experiments under controlled pH, temperature and precipitation rate. *Geochimica et Cosmochimica Acta* **150**, 299–313.
- McCoy S. J., Robinson L. F., Pfister C. A., Wootton J. T. and Shimizu N. (2011) Exploring B/Ca as a pH proxy in bivalves: relationships between *Mytilus californianus* B/Ca and environmental data from the northeast Pacific. *Biogeosciences* **8**, 2567–2579.
- McClaine, L.A., Bullwinkel, E.P., Huggins, J.C., 1955. The carbonate chemistry of uranium. Theory and Application. In: Proceeding of the Conference on the Peaceful Use of the Atomic Energy, vol. 8, pp. 26–37.

- McCulloch Malcol, Trotter Juli, Montagna Paol, Falter Ji, Dunbar Rober, Freiwald André, Försterra Günte, Correa Matthias López, Maier Corneli, Rüggeberg Andre and Taviani Marc (2012) Resilience of cold-water scleractinian corals to ocean acidification: Boron isotopic systematics of pH and saturation state up-regulation. *Geochimica et Cosmochimica Acta* **87**, 21–34.
- Meece D. E. and Benninger L. K. (1993) The coprecipitation of Pu and other radionuclides with CaCO₃. *Geochim. Cosmochim. Acta* **57**, 1447–1458.
- Misogianes M. J. and Chasteen N. D. (1979) A chemical and spectral characterization of the extrapallial fluid of *Mytilus edulis*. *Anal. Biochem.* **100**, 324–334.
- Mucci A. and Morse J. W. (1983) The incorporation of Mg²⁺ and Sr²⁺ into calcite overgrowths: influences of growth rate and solution composition. *Geochim. Cosmochim. Acta* **47**, 217–233.
- Nehrke G., Keul N., Langer G., de Nooijer L. J., Bijma J. and Meibom A. (2013) A new model for biomineralization and trace element signatures of Foraminifera tests. *Biogeosciences* **10**, 6759–6767.
- Nollet L. M. L. and De Gelder L. S. P. (2013) *Handbook of Water Analysis*, third ed. CRC Press, Taylor & Francis Group, Boca Raton, USA.
- Okumura M. and Kitano Y. (1986) Coprecipitation of alkali metal ions with calcium carbonate. *Geochim. Cosmochim. Acta* **50**, 49–58.
- Planchon F., Poulain C., Langlet D., Paulet Y. M. and André L. (2013) Mg-isotopic fractionation in the manila clam (*Ruditapes philippinarum*): new insights into Mg incorporation pathway and calcification process of bivalves. *Geochim. Cosmochim. Acta* **121**, 374–397.
- Rodolfo-Metalpa R., Houlbrequé F., Tambutte E., Boisson F., Baggini C., Patti F. P., Jeffree R., Fine M., Foggo A., Gattuso J.-P. and Hall-Spencer J. M. (2011) Coral and mollusc resistance to ocean acidification adversely affected by warming. *Nat. Clim. Change* **1**(6), 308–312.
- Rosenheim B. E., Swart P. K. and Thorrold S. R. (2005) Minor and trace elements in sclerosponge *Ceratoporella nicholsoni*: biogenic aragonite near the inorganic endmember? *Palaeogeogr. Palaeoclimatol. Palaeoecol.* **228**, 109–129.
- Russell A. D., Hönisch B., Spero H. J. and Lea D. W. (2004) Effects of seawater carbonate ion concentration and temperature on shell U, Mg, and Sr in cultured planktonic foraminifera. *Geochim. Cosmochim. Acta* **68**(21), 4347–4361.
- Schifano G. (1984) Environmental, biological, and mineralogical controls on strontium incorporation into skeletal carbonates in some intertidal gastropod species. *Palaeogeogr. Palaeoclimatol. Palaeoecol.* **46**, 303–312.
- Schöne B. R., Zhang Z., Radermacher P., Thébault J., Jacob D. E., Nunn E. V. and Maurer A.-F. (2011) Sr/Ca and Mg/Ca ratios of ontogenetically old, long-lived bivalve shells (Arctica islandica) and their function as paleotemperature proxies. *Palaeogeogr. Palaeoclimatol. Palaeoecol.* **302**, 52–64.
- Shen G. T. and Dunbar R. B. (1995) Environmental controls on uranium in reef corals. *Geochim. Cosmochim. Acta* **59**, 2009–2024.
- Simkiss K. and Wilbur K. (1989) *Biomineralization* (1989) *Cell Biology and Mineral Deposition*. Academic Press, San Diego.
- Sosdian S., Gentry D. K., Lear C. H., Grossman E. L., Hicks D. and Rosenthal Y. (2006) Strontium to calcium ratios in the marine gastropod *Conus ermineus*: growth rate effects and temperature calibration. *Geochem. Geophys. Geosyst.* **7**, Q11023. <https://doi.org/10.1029/2005GC001233>.
- Stoll, Heather, Langer, Gerald, Shimizu, Nobumichi, Kanamaru, Kinuyo, 2012. B/Ca in coccoliths and relationship to calcification vesicle pH and dissolved inorganic carbon concentrations. In: *Geochimica et Cosmochimica Acta*, vol. 80, pp. 143–157, ISSN 0016-7037, <https://doi.org/10.1016/j.gca.2011.12.003>.
- Suzuki M., Saruwatari K., Kogure T., Yamamoto Y., Nishimura T., Kato T. and Nagasawa H. (2009) An acidic matrix protein, Pif, is a key macromolecule for nacre formation. *Science* **325**, 1388–1390.
- Swart P. K. and Hubbard J. A. E. B. (1982) Uranium in scleractinian coral skeletons. *Coral Reefs* **1**, 13–19.
- Sunday J. M., Fabricius K. E., Kroeker K. J., Anderson K. M., Brown N. E., Barry J. P., Connell S. D., Dupont S., Gaylord B., Hall-Spencer J. M., Klinger T., Milazzo M., Munday P. L., Russell B. D., Sanford E., Thiagarajan V., Vaughan M. L. H., Widdicombe S. and Harley C. D. G. (2017) Ocean acidification can mediate biodiversity shifts by changing biogenic habitat. *Nat. Clim. Change* **7**, 81–85.
- Takesue R. K. and van Green A. (2004) Mg/Ca, Sr/Ca, and stable isotopes in modern and Holocene *Protothaca staminea* shells from a northern California coastal upwelling region. *Geochim. Cosmochim. Acta* **68**, 3845–3861.
- Tambutté E. et al. (2012) Calcein labelling and electrophysiology: insights on coral tissue permeability and calcification. *Proc. Biol. Sci.* **279**, 19–27.
- Tang J., Koehler S. J. and Dietzel M. (2008) Sr²⁺/Ca²⁺ and 44Ca/40Ca fractionation during inorganic calcite formation: I. Sr incorporation. *Geochim. Cosmochim. Acta* **72**, 3718–3732.
- Taylor Alison R., Brownlee Coli and Wheeler Gle (2017) Coccolithophore cell biology: chalking up progress. *Annu. Rev. Mar. Sci.* **9**, 283–310.
- Tesoriero A. J. and Pankow J. F. (1996) Solid solution partitioning of Sr²⁺, Ba²⁺, and Cd²⁺ to calcite. *Geochim. Cosmochim. Acta* **60**, 1053–1063.
- Thébault J., Schöne B. R., Hallmann N., Barth M. and Nunn E. V. (2009) Investigation of Li/Ca variations in aragonitic shells of the ocean quahog *Arctica islandica*, northeast Iceland. *Geochem. Geophys. Geosyst.* **10**, Q12008. <https://doi.org/10.1029/2009GC002789>.
- Uchikawa J., Penman D. E., Zachos J. C. and Zeebe R. E. (2015) Experimental evidence for kinetic effects on B/Ca in synthetic calcite: Implications for potential B(OH)₄⁻ and B(OH)₃ incorporation. *Geochim. Cosmochim. Acta* **150**, 171–191.
- Ullmann C. V., Böhm F., Rickaby R. E. M., Wiechert U. and Korte C. (2013) The giant pacific oyster (*Crassostrea gigas*) as a modern analog for fossil ostreoids: isotopic (Ca, O, C) and elemental (Mg/Ca, Sr/Ca, Mn/Ca) proxies. *Geochem. Geophys. Geosyst.* **14**, 4109–4120.
- Vidavsky N. et al. (2016) Calcium transport into the cells of the sea urchin larva in relation to spicule formation. *Proc. Natl. Acad. Sci. USA* **113**, 12637–12642.
- Watabe N. and Wilbur K. M. (1960) Influence of the organic matrix on crystal type in molluscs. *Nature* **188**, 334.
- Xiang L., Kong W., Su J., Liang J., Zhang G. and Xie L., et al. (2014) Amorphous calcium carbonate precipitation by cellular biomineralization in mantle cell cultures of pinctada fucata. *PLoS ONE* **9**(11), e113150. <https://doi.org/10.1371/journal.pone.0113150>.
- Yu J., Elderfield H. and Hönisch B. (2007) B/Ca in planktonic foraminifera as a proxy for surface seawater pH. *Paleoceanography* **22**, PA2202. <https://doi.org/10.1029/2006PA001347>.
- Yu J., Elderfield H., Jin Z., Tomascek P. and Rohling E. J. (2014) Controls on Sr/Ca in benthic foraminifera and implications for seawater Sr/Ca during the late Pleistocene. *Quat. Sci. Rev.* **98**, 1–6.
- Zhong S. and Mucci A. (1989) Calcite and aragonite precipitation from seawater solutions of various salinities: precipitation rates and overgrowth compositions. *Chem. Geol.* **78**, 283–299.

Associate editor: Thomas M. Marchitto